

Multiresponsive luminescent metal–organic framework for cooking oil adulteration detection and gallium(III) sensing



Dmitry I. Pavlov ^{a,b,1}, Xiaolin Yu ^{a,b,1}, Alexey A. Ryadun ^a, Denis G. Samsonenko ^a, Pavel V. Dorovatovskii ^c, Vladimir A. Lazarenko ^c, Na Sun ^d, Yaguang Sun ^d, Vladimir P. Fedin ^{a,b}, Andrei S. Potapov ^{a,b,*}

^a Novosibirsk State University, 2 Pirogov Str., 630090 Novosibirsk, Russia

^b Nikolaev Institute of Inorganic Chemistry, Siberian Branch of the Russian Academy of Sciences, 3 Lavrentiev Ave., 630090 Novosibirsk, Russia

^c National Research Centre "Kurchatov Institute", Kurchatov Square 1, Moscow 123182, Russia

^d Key Laboratory of Inorganic Molecule-Based Chemistry of Liaoning Province, Shenyang University of Chemical Technology, Shenyang 110142, China

ARTICLE INFO

Keywords:

Gossypol
Metal–organic framework
Luminescent sensor
Gallium
Benzothiadiazole
Oil adulteration

ABSTRACT

A new 3D metal–organic framework $\{[\text{Cd}_{16}(\text{tr}_2\text{btd})_{10}(\text{dcddps})_{16}(\text{H}_2\text{O})_3(\text{EtOH})]\bullet15\text{DMF}\}_n$ (**MOF 1**, $\text{tr}_2\text{btd} = 4,7\text{-di}(1,2,4\text{-triazol-1-yl})\text{benzo-2,1,3-thiadiazole}$, $\text{H}_2\text{dcddps} = 4,4'\text{-sulfonyldibenzoic acid}$) was obtained and its luminescent properties were studied. **MOF 1** exhibited bright blue-green luminescence with a high quantum yield of 74 % and luminescence quenching response to a toxic natural polyphenol gossypol and luminescence enhancement response to some trivalent metal cations (Fe^{3+} , Cr^{3+} , Al^{3+} and Ga^{3+}). The limit of gossypol detection was 0.20 μM and the determination was not interfered by the components of the cottonseed oil. The limit of detection of gallium(III) was 1.1 μM . It was demonstrated that **MOF 1** may be used for distinguishing between the genuine sunflower oil and oil adulterated by crude cottonseed oil through qualitative luminescent and quantitative visual gossypol determination.

1. Introduction

Vegetable oils are used in cooking as a base for frying, stewing and baking, in cosmetology as components of creams, lotions and massage oils, medicine and other fields. The most widespread types of edible vegetable oils include olive, sunflower, coconut, cottonseed and sesame oils (Stefanidis et al., 2023; Tian et al., 2023).

Sunflower oil is one of the most popular types of vegetable oils, which is used for cooking fried dishes, baking, salad dressing and other culinary purposes. It has a high smoking temperature and it does not lose its properties when heated. The sunflower oil world production constituted 20,141 millions of tons in 2022, which corresponds to about 8 % of all edible oil consumption (Puttha et al., 2023).

Adulteration of sunflower oil is a well-known problem of the edible oil market and, as a rule, it involves the dilution of sunflower oil with cheaper oils, such as cottonseed oil (Tan et al., 2021). Although mixing of food-grade high quality oils does not pose any health-related issues

and even may be used in culinary experiments to create unique flavor combinations and textures, the oil used for adulteration is often of substandard quality and may have elevated gossypol content.

Gossypol is a natural product that cotton plants produce to protect themselves from insect pests and it is concentrated mostly in seeds and leaves. A by-product of cotton production is cottonseed meal – a valuable source of fats and proteins for livestock (Kumar et al., 2021; Raj et al., 2023; Xu et al., 2024). However, its use as animal feed is limited by the toxicity of gossypol. Some cotton species produce so much gossypol that its content may reach 34 g of gossypol per 1 kg of cottonseeds (Percy et al., 1996). As gossypol is insoluble in water, but partly soluble in fats and oils, unrefined cottonseed oil contains significant quantities of gossypol. Gossypol is highly toxic to humans, with the exposure effects including hepatotoxicity, infertility and immunotoxicity (Lin et al., 2023; Liu et al., 2022). A clinical trial in China found that out of all volunteers consuming just 50 mg/week of gossypol for 1 year 10 % developed irreversible aspermatogenesis (Dodou, 2005). Despite

* Corresponding author at: Nikolaev Institute of Inorganic Chemistry, Siberian Branch of the Russian Academy of Sciences, 3 Lavrentiev Ave., 630090 Novosibirsk, Russia.

E-mail address: potapov@niic.nsc.ru (A.S. Potapov).

¹ The authors contributed equally.

the fact that methods to reduce the free gossypol content in cottonseed exit, they involve complicated techniques, including production of genetically engineered cotton or extraction of cottonseeds by organic solvents of porous adsorbents (Dabbour et al., 2023; Kumar et al., 2023; Ninkuu et al., 2023; Wang et al., 2023). Both approaches increase the cost of oil manufacture, raise environmental concerns, and often not employed in functioning agricultural companies. For areas where cottonseed oil is consumed on a daily basis this poses a significant risk for people, who suffer serious consequences resulting from chronic gossypol exposure (Gadelha et al., 2014). The Chinese Ministry of Health limited the allowed quantity of free gossypol in cottonseed cooking oil at 200 ppm (GB 2716–2018. National food safety standard - Vegetable oil, 2018), while the EU regulators allow the concentrations from 20 to 5000 ppm for various animal feed materials (Directive, 2002/32/EC of the European Parliament and of the Council of 7 May 2002 on undesirable substances in animal feed - Council statement, 2002).

Recently, there were several reports on sunflower oil adulteration in Xinjiang province of People's Republic of China, where raw cottonseed oil was used to dilute pure sunflower oil (Yili Prefecture Market Supervision and Administration Bureau Administrative Penalty Decision Letter Yizhou City Supervision Penalty [2022] No. 27, 2022). Edible oil adulteration by mixing with cottonseed oil can pose a danger to the population, as the sunflower oil is never tested for the presence of gossypol. Consequently, there exists a pressing demand for the development of accessible and efficient methodologies to identify gossypol in various oils.

Currently luminescent sensing of organic and inorganic pollutants using metal-organic frameworks (MOFs) is intensively developing and offers high sensitivity, selectivity and the possibility of creating portable devised for field operation (Agafonov et al., 2022; Cai et al., 2023; Guan et al., 2021; Liu et al., 2019; Ma et al., 2013; Mohan et al., 2023; Pavlov et al., 2023; Yang et al., 2023; Yu et al., 2022a; Yu et al., 2022b; Yu et al., 2023a; Yu et al., 2023b). Recently we have demonstrated that a MOF built using benzo-2,1,3-thiadiazole-derived linkers with imidazole moieties was able to detect gossypol in submicromolar concentrations through the luminescence quenching effect (Pavlov et al., 2023).

Extending our studies to other benzo-2,1,3-thiadiazole-based ligands, we have designed a new metal-organic framework based on 4,7-di(1,2,4-triazol-1-yl)benzo-2,1,3-thiadiazole (tr_2btd) and 4,4'-sulfonyldibenzoinic acid (H_2dcfps) ligands with improved gossypol sensitivity and hypothesized that by detecting gossypol in the samples of sunflower oils it is possible to distinguish genuine product from the one adulterated

by adding the cottonseed oil (Scheme 1). Approaches to detect oil adulteration through specific component monitoring are known from the literature, but they involve complicated and expensive techniques such as NMR (Giebelhaus et al., 2023), SERS (Yao-Say Solomon Adade et al., 2022), FT-IR (Salah & Nofal, 2021; Vilela et al., 2015) or UV-Vis spectroscopy (Muthukumar et al., 2021; Zaukuu et al., 2024), gas chromatography (Yakar & Karadag, 2022) or differential pulse voltammetry (Lyu et al., 2023) and no methods used gossypol as fraud marker.

Industrial use of gallium has significantly increased in the past 40 years. Gallium is used primarily as a component of integrated circuits and optoelectronic devices (Hu et al., 2023; Zhan et al., 2023). Gallium is also used in nuclear medicine, where the isotopes ^{67}Ga and ^{68}Ga act as imaging agents (Chitambar, 2010; Li et al., 2023; Rizzo et al., 2023). Due to the rapidly increasing gallium use, gallium exposure is increasing, especially in occupational settings (Ivanoff et al., 2012; Li et al., 2024). Some animal studies and investigation of gallium compounds as chemotherapeutic agents suggest a notable level of toxicity to the vertebrates. It is vital to acknowledge that lack of regulation does not translate into the lack of toxicity (White & Shine, 2016). Since the long-term exposure effects are poorly understood, care should be taken to limit the gallium exposure. To achieve this, additional measures for the detection and quantification of gallium content in the environment should be developed.

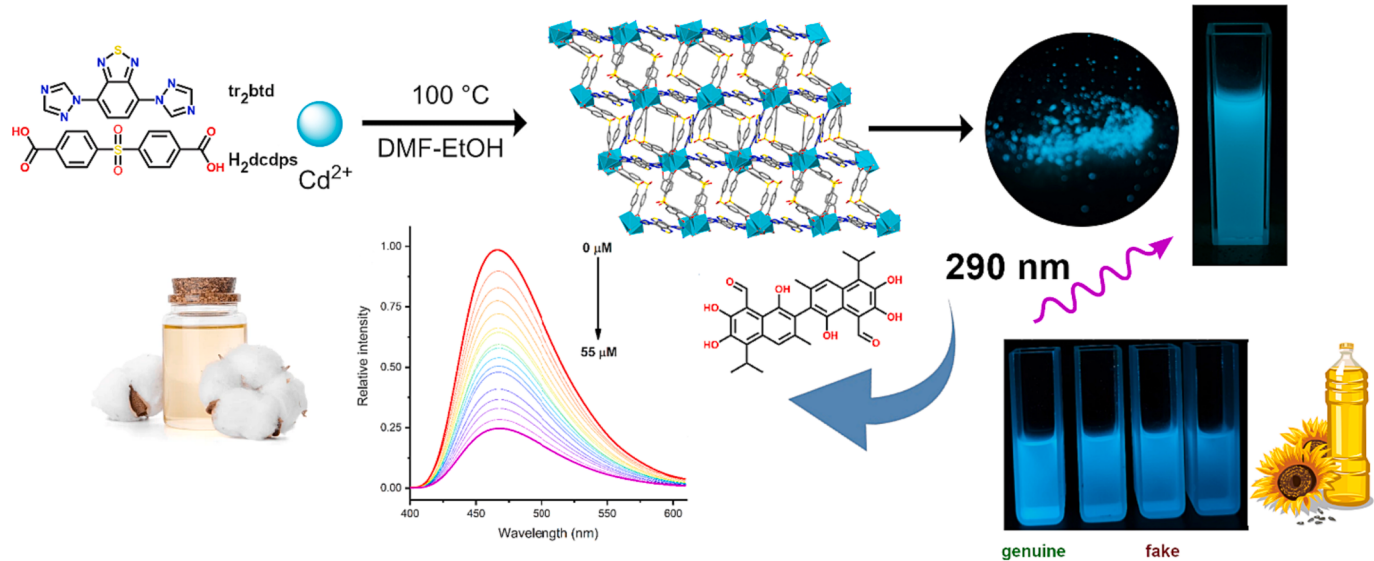
The possibility of detecting metal cations using MOFs containing benzo-2,1,3-thiadiazole units was demonstrated in several recent works (Chai et al., 2022; He et al., 2022; Li et al., 2022a; Li et al., 2021; Li et al., 2022; Pavlov et al., 2021; Tian et al., 2020; Yao et al., 2021). We have studied the sensing properties MOF 1 towards Ga^{3+} cations and found a luminescence turn-on response with the limit of detection of 1.1 μM , which is among the best values reported so far.

2. Experimental section

4,7-Di(1,2,4-triazol-1-yl)benzo-2,1,3-thiadiazole (tr_2btd) was prepared as described previously (Pavlov et al., 2021). Other commercially available chemicals were used as received.

2.1. Synthesis of $\{[\text{Cd}_{16}(\text{tr}_2\text{btd})_{10}(\text{dcfps})_{16}(\text{H}_2\text{O})_3(\text{EtOH})]\bullet15\text{DMF}\}_n$ (MOF 1)

Two portions (5 mL each) of solution of tr_2btd (50 mg, 0.185 mmol),



Scheme 1. Synthesis and application of MOF 1 for gossypol detection and sunflower oil authenticity determination.

H_2dcdps (57 mg, 0.185 mmol) and $\text{Cd}(\text{NO}_3)_2 \cdot 4\text{H}_2\text{O}$ (57 mg, 0.185 mmol) in 10 mL of DMF:EtOH (3:1) were placed in two 20 mL screwcap vials and heated at 100 °C for 48 h. Transparent block crystals with a green tint were filtered, washed with DMF and ethanol and dried on air. Yield 73 % (yellow-green crystals). Elemental analysis found (%): C 41.8, H 2.7, N 12.2, S 8.0, calculated for $\text{C}_{371}\text{H}_{305}\text{Cd}_{16}\text{N}_{95}\text{O}_{115}\text{S}_{26}$ (%): C 42.17, H 2.91, N 12.59, S 7.89. IR (cm^{-1}): 3392 (m), 3140 (m), 2926 (w), 1676 (s), 1600 (s), 1558 (s), 1406 (s), 1298 (s), 1166 (s), 1108 (s), 981 (m), 848 (m), 742 (s), 621 (w).

2.2. Physicochemical methods of analysis

Elemental analysis (CHNS) was carried out on a Vario MICRO Cube Analyzer. The FT-IR spectra were recorded on a Bruker Scimitar FTS 2000 spectrometer in KBr pellets. Thermogravimetric analysis was conducted on a NETZSCH TG 209 F1 Iris Thermo Microbalance in a helium atmosphere. The UV-Vis absorption spectra were recorded on SF-2000 spectrophotometer. Powder X-ray diffraction measurements were performed on a Bruker D8 ADVANCE diffractometer. Gas adsorption studies were carried out on an Autosorb iQ instrument. Luminescence spectra were acquired using HORIBA Fluorolog 3 spectrofluorimeter.

Ethanol suspension of **MOF 1** was prepared following a conventional protocol (Han et al., 2023). Specifically, 20 mg of finely powdered **MOF 1** were ultrasonically dispersed in 20 mL of ethanol. For the luminescence measurements, 500 μL of the prepared suspension was diluted by ethanol to 2 mL in 1 cm quartz cuvette. The sensing performance of **MOF 1** towards gossypol in ethanol suspension and cottonseed oil samples was studied at 290 nm excitation wavelength. The analysis of sunflower seed oil samples was carried out at 315 nm excitation wavelength, which was found to be optimal in terms of sensitivity for this matrix.

The limits of detection (LODs) were calculated as $3\sigma/k$, where k is the slope of the I - C correlation, and σ is the standard deviation calculated from ten successive blank measurements (Committee, 1987).

For oil sample analyses, gossypol solutions in sunflower oil with concentration of 200 ppm were prepared. A portion of 10 μL of this solution oil was added to the **MOF 1** suspension in a quartz cuvette and was stirred thoroughly. After the measurement, an additional quantity of gossypol was introduced as a solution in ethanol, and the recovery was calculated.

The screening of the luminescent response to metal cations was carried out by mixing 20 μL aliquots of aqueous metal nitrate solutions (NaNO_3 , $\text{Mg}(\text{NO}_3)_2$, $\text{Cu}(\text{NO}_3)_2$, $\text{Zn}(\text{NO}_3)_2$, $\text{Cd}(\text{NO}_3)_2$, $\text{Ni}(\text{NO}_3)_2$, $\text{Co}(\text{NO}_3)_2$, $\text{Fe}(\text{NO}_3)_3$, $\text{Al}(\text{NO}_3)_3$, $\text{Ga}(\text{NO}_3)_3$, $\text{Cr}(\text{NO}_3)_3$, $\text{La}(\text{NO}_3)_3$, C 0.01 M), 1.48 mL of ethanol and 0.5 mL of **MOF 1** ethanol suspension to create $1 \cdot 10^{-4}$ M concentration of metal cations in 1 cm quartz cuvette. The indicated sequence of adding the solutions was followed to avoid contact of **MOF 1** with undiluted aqueous solutions. For interference experiments, equal concentrations ($1 \cdot 10^{-4}$ M) of the analyzed cations (Fe^{3+} , Al^{3+} , Cr^{3+} or Ga^{3+}) and potentially interfering cations were created in **MOF 1** ethanol suspension as described above.

Fluorometric titration of Ga^{3+} was carried out by adding aliquots of $1 \cdot 10^{-4}$ M $\text{Ga}(\text{NO}_3)_3$ aqueous solution to a mixture of 1.5 mL of ethanol and 0.5 mL of **MOF 1** ethanol suspension in 1 cm quartz cuvette.

For all metal sensing experiments the luminescence spectra were recorded using 375 nm excitation wavelength and integral emission intensity (from 400 to 670 nm) was used in all plots and calculations.

2.3. X-ray crystal structure analysis

Diffraction data for single crystals of **MOF 1** were obtained on the “Belok/XSA” beamline (Lazarenko et al., 2017; Svetogorov et al., 2020) ($\lambda = 0.7527 \text{ \AA}$) of the National Research Center “Kurchatov Institute” (Moscow, Russian Federation) using a Rayonix SX165 CCD detector. The data were indexed, integrated and scaled, and absorption correction was applied using the XDS program package (Kabsch, 2010b, 2010a). The

structures were solved by the dual-space algorithm using SHELXT software (Sheldrick, 2015b) and refined by the full-matrix least-squares technique in SHELXL package (Sheldrick, 2015a) in the anisotropic approximation (except hydrogen atoms). Positions of the hydrogen atoms were calculated geometrically and refined in the riding model.

Crystal data for MOF 1: $\text{C}_{371}\text{H}_{305}\text{Cd}_{16}\text{N}_{95}\text{O}_{115}\text{S}_{26}$ ($M = 10566.04 \text{ g/mol}$): triclinic, space group $P-1$, $a = 15.3880(18) \text{ \AA}$, $b = 26.9420(15) \text{ \AA}$, $c = 27.6530(18) \text{ \AA}$, $\alpha = 108.613(6)^\circ$, $\beta = 100.722(4)^\circ$, $\gamma = 104.980(12)^\circ$. $V = 10033.9(16) \text{ \AA}^3$, $Z = 1$, $T = 100(2) \text{ K}$, $D_{\text{calc}} = 1.749 \text{ g/cm}^3$, 62,009 reflections measured, 37,579 unique ($R_{\text{int}} = 0.040$, $R_{\text{sigma}} = 0.049$). The final R_1 [$I > 2\sigma(I)$] 0.037, goodness of fit $S = 1.040$, wR_2 (all data) 0.094. CCDC deposition number 2310836.

3. Results and discussion

3.1. Synthesis and crystal structure

MOF 1 was obtained in high yield (73 %) in one step by reacting equimolar amounts of tr_{2}btd , H_2dcdps and $\text{Cd}(\text{NO}_3)_2 \cdot 4\text{H}_2\text{O}$ in the mixed solvent DMF:EtOH (3:1) at 100 °C. Both phase and chemical purity were confirmed by PXRD, TGA, elemental analysis and IR spectroscopy (Figures S1, S2).

According to single-crystal X-Ray diffraction analysis, **MOF 1** crystallizes in a triclinic crystal system, $P-1$ space group (Fig. 1a). The asymmetric unit of **MOF 1** contains eight crystallographically independent Cd^{2+} cations, seven of which are in a distorted octahedral arrangement and one exhibits a distorted pentagonal bipyramidal geometry. There are five crystallographically independent tr_{2}btd ligands and eight dcdps^{2-} anions with slight conformational differences in the asymmetric unit (Figure S3).

The secondary building unit (SBU) of **MOF 1** can be represented by four Cd^{2+} cations, bridged by the carboxylate groups of dcdps^{2-} ligands (Fig. 1b). Each SBU has thirteen extension points, by which it is joined to six other SBUs to form a 3D framework. To the best of our knowledge, such 13-connected SBU was never encountered before in MOF crystal structures (Butova et al., 2016; Tranchemontagne et al., 2009). According to ToposPro program (Blatov et al., 2014; Bonneau et al., 2018), the framework may be described as a dense six-connected uninodal net with point symbol $3^3 \bullet 4^6 \bullet 5^5 \bullet 6$, topological type **sxd** (Barthel et al., 2018) (Fig. 1c). The framework features two types of one-dimensional channels propagating along the crystallographic axis a (Fig. 1c). The channel dimensions are $3.3 \times 3.0 \text{ \AA}$ and $3.0 \times 2.0 \text{ \AA}$. In the as-synthesized MOF, the channels are filled with DMF molecules. The solvent-accessible volume is 20 % as estimated by PLATON software (Spek, 2015). It is interesting to note that the “walls” of the channels are formed only by the phenyl rings of the dcdps^{2-} ligand (Fig. 1c), thus the 2,1,3-benzothiadiazole fragments are inaccessible to any guest molecules. There is an extensive network of short intermolecular contacts, and 2,1,3-benzothiadiazole moieties in different ligand molecules of the asymmetric unit are interacting with CH fragments, N, O, and C atoms of the neighboring ligands. Chalcogen-pnictogen (S···N,N,N) contacts between the 2,1,3-benzothiadiazole fragments and the 1,2,4-triazole rings of the neighboring ligands (Figure S4) are the most significant and are likely to determine the conformational rigidity of tr_{2}btd ligands. The average S–N internuclear distance is 3.212 \AA , which is less than the sum of Van-der-Walls radii of sulfur and nitrogen atoms by about 0.14 \AA .

Despite the fact that both types of ligands contain aromatic cycles and are closely located in the structure of **MOF 1**, no π - π stacking interactions were found, which, along with the conformational rigidity of tr_{2}btd , may be the reason for an exceptionally high photoluminescence quantum yield of **MOF 1**.

3.2. Phase purity, thermal stability and textural properties of **MOF 1**

To evaluate the phase purity of the bulk product and its stability in different solvents, a powder X-ray diffraction (PXRD) method was

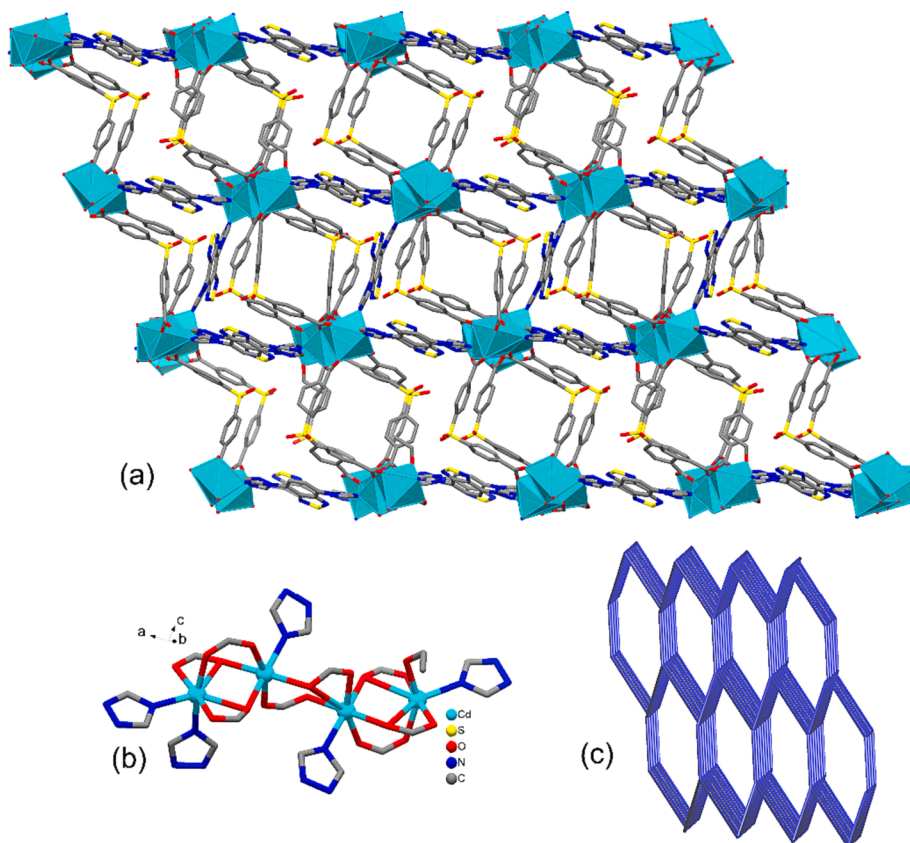


Fig. 1. Crystal structure of **MOF 1**: (a) 3D framework structure; (b) 13-connected secondary building unit; (c) topological representation of the framework connectivity.

applied. The analysis indicates that the bulk powder of **MOF 1** is phase-pure (Figure S1). The chemical composition of **MOF 1** determined from single-crystal X-Ray diffraction data corresponds well to the results of the elemental (CHNS) analysis.

In addition, thermogravimetric analysis (TGA) was used to estimate the thermal stability of **MOF 1** and the possibility of activation for gas adsorption studies. **MOF 1** demonstrated a mass loss (Δm 10 %) in the temperature range 110–200 °C (Figure S5), attributed to removal of solvent molecules from the channels (calculated Δm 10.4 % for 15 DMF molecules). After removal of solvent molecules, no mass change or thermal effects were observed up to 315 °C and at higher temperature (345 °C) a quick degradation takes place (Figure S5). No significant mass changes for the activated sample of **MOF 1** were observed in the temperature range 80–315 °C (Figure S5), thus it can be concluded that **MOF 1** is thermally stable up to this temperature and may be activated for evaluation of the porous structure parameters.

For the gas adsorption measurements, samples of as-synthesized **MOF 1** were activated as described in the Experimental part. The adsorption–desorption isotherms (Figure S6) for nitrogen (at 77 K) and carbon dioxide (at 195 K) belong to type I according to IUPAC classification, characteristic of microporous compounds (Sing et al., 1985). The specific surface area (S_{BET}) was determined to be 330 m²/g. The measured pore volume was 0.222 cm³/g, which is in good agreement with the value of 0.239 cm³/g calculated from the SCXRD data. Interestingly, a higher uptake of N₂ than CO₂ was observed, which is an unusual adsorption behavior. This may be explained by the fact that polar 2,1,3-benzothiadiazole fragments are isolated from the channel surface and thus cannot enhance of the CO₂ adsorption in narrow channels.

3.3. Luminescent and sensing properties of **MOF 1**

Assessment of **MOF 1** stability through immersion in various solvents revealed that the compound is stable in common organic solvents, yet a degradation process was observed in water (Fig. 2a).

The photoluminescent properties of **MOF 1** were examined both in the solid state and in ethanol suspension. Compared to the emission of tr₂btd ligand, which exhibited a maximum at 515 nm ($\lambda_{\text{ex}} = 404$ nm), **MOF 1** displayed the emission maximum at 470 nm (Fig. 2b), which constitutes a 45 nm hypsochromic shift. The shift of the emission maximum relative to the free ligand may be attributed to the difference in tr₂btd conformations in the free state and in the structure of **MOF 1**. Thus, the dihedral angles between the 1,2,4-triazole and the phenyl ring in tr₂btd in the solid state are 161.5(7)° and 172.4(6)° (Table S1). In the structure of **MOF 1** tr₂btd ligands are represented by a set of conformations. The absolute values of the dihedral angles corresponding to the rotation of 1,2,4-triazole rings relative to the benzene rings in five crystallographically independent molecules are in the range of 138.8(5)–172.1(5)° with two instances of almost inverse orientation of 1,2,4-triazole rings with the dihedral angles of 21.1(8)° and 18.9(9)° (Table S1). Different conformations lead to a variation in the energy difference between the ground and the excited states resulting in different emission maxima. The luminescence quantum yield is 74 %, which is the highest among MOFs containing benzo-2,1,3-thiadiazole moiety (Kuznetsova et al., 2020) and one of the highest values for transition-metal-based MOFs (Barsukova et al., 2018; Kokina et al., 2023).

3.3.1. Sensing of gossypol in cottonseed and sunflower oils

In order to evaluate the luminescent response of **MOF 1** to gossypol (GOS) an aliquot of its solution was added to the ethanol suspension of **MOF 1** to create a 55 μM concentration. The strongest luminescence quenching (monitored at 470 nm) was observed for 290 nm excitation

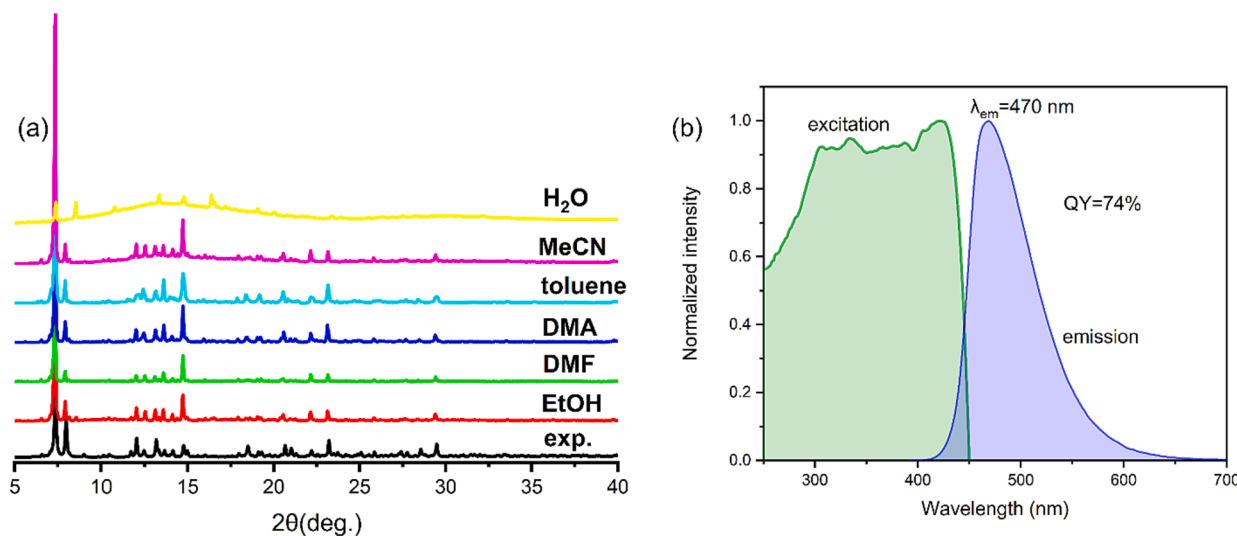


Fig. 2. (a) PXRD patterns of **MOF 1** after soaking for 24 h in different solvents. (b) Solid-state emission (λ_{ex} 290 nm) and excitation (λ_{em} 470 nm) spectra of **MOF 1**.

wavelength, at which the quenching degree reached 75 % (Fig. 3a).

Fluorometric titration demonstrated a concentration-dependent emission quenching with a linear range 0.15–1.0 μM (Fig. 3b) and the limit of detection of gossypol as low as 0.20 μM . To the best of our knowledge, the found value is one of the lowest among the reported transition metal-based MOFs responsive to gossypol through the luminescence quenching mechanism (Table S2) (W. Li et al., 2024; Pavlov et al., 2023).

In order to examine the potential application of **MOF 1** as a sensor for detecting gossypol in cottonseed oil samples, we conducted the fluorometric titration as described above. A fixed quantity of refined cottonseed oil was introduced into the suspension as a background, which allowed for the assessment of the interference arising from multiple oil components, such as triglycerides, terpenoids, phospholipids, etc. (Tian et al., 2023; Ye et al., 2022). Experiment revealed a discernible emission quenching upon the addition of cottonseed oil to the suspension (Figure S7). Despite this, the concentration-intensity dependence remained linear, and conformed to the equation with analogous parameters, and the LOD was ascertained at 0.12 μM (Fig. 3c, Figure S8). Therefore, linear calibration plots can be obtained even in the presence of cottonseed oil, which renders **MOF 1** suitable for the quantitative determination of gossypol in real-life samples.

To evaluate our hypothesis that **MOF 1** may be used for differentiation between the genuine and adulterated sunflower oil, samples of sunflower seed oil contaminated with a known amount of gossypol (200 ppm) were prepared. It was found that, unlike cottonseed oil, addition of sunflower seed oil did not change the luminescence intensity of the suspension. The optimal excitation wavelength for the quenching response in these conditions was found to be 315 nm. Spiking experiment was designed in which 10 μL of gossypol-contaminated sunflower oil were added to the blank **MOF 1** suspension, the luminescence spectrum was recorded, then a standard solution of gossypol in ethanol was added, the luminescence spectrum was recorded again and the concentration of gossypol was calculated from the difference in the luminescence intensities (relative to the blank suspension). Over five separate measurements the average calculated concentration was 207 ppm, which gives a good recovery value of 104 % and RMSD of 22 % (Table S3). Therefore, **MOF 1** may be used as a sensor for quantitative determination of gossypol in cooking oil samples in a concentration range encountered in real-life samples.

We have also demonstrated the possibility of a simple visual discrimination between the genuine and adulterated sunflower oil. To the ethanol suspension of **MOF 1** a series of sunflower oil samples were added, which contained different concentration of gossypol (50, 100,

200 ppm), thus modeling sunflower oil adulterated by addition of crude cottonseed oil. The difference in the emission intensity under a conventional 254 nm UV lamp was visible even for 50 ppm gossypol content (Fig. 3d) thus confirming the possibility of a facile visual detection of adulterated sunflower oil without using any special equipment.

Therefore, the hypothesis was confirmed and **MOF 1** may be used for both quantitative determination of gossypol in edible oils and visual qualitative detection of adulterated sunflower oil.

One notable advantage that metal-organic frameworks (MOFs) offer over conventional sensing methods utilizing homogenous systems lies in their capacity for regeneration and repeated utilization. The reusability of **MOF 1** in gossypol sensing was explored by repeating the cycles in which the solid **MOF 1** was separated from the suspension by centrifugation, thoroughly washed and resuspended for the next sensing cycle. It was found that the sensing response is reversible and **MOF 1** can be recycled several times without any loss of sensitivity (Figure S9).

3.3.2. Sensing of metal cations

To expand the sensing properties of **MOF 1** its luminescence spectra were evaluated for ethanol suspensions containing different metal nitrates (concentration 0.1 mM). The luminescence intensity exhibited virtually no dependence on the presence of the majority of metal cations, with the exception of Ga³⁺, Al³⁺, Fe³⁺, and Cr³⁺ (Fig. 4a). Addition of these metals resulted in a luminescence “turn-on” effect, as well as a bathochromic shift of the emission maximum by 20 nm (Figure S10). The most pronounced effect was observed for Ga³⁺ cations which caused more than a two-fold luminescence intensity increase, compared to the blank experiment. Interference experiments were conducted for all of four mentioned metal cations. When Ga³⁺ was added to the solution in pair with each of the other metal cations in equal concentrations, no notable change in the luminescence enhancement degree was observed, except for the quenching effect of Cu²⁺ (Fig. 4b). A similar behavior was observed for Fe³⁺ ions, but in this case a significant quenching upon addition of the Mg²⁺ ions was also noted (Figure S11). In case of metal interfering experiments with Al³⁺, a strong quenching effect of Cu²⁺ was also observed, without any significant change in case of other ions (Figure S12). Finally, several metal ions interfered with the detection of Cr³⁺ ions, namely In³⁺, Ga³⁺, Al³⁺, Fe³⁺ (Figure S13). Therefore, it may be concluded that **MOF 1** is a potential candidate for the selective detection of Ga³⁺ and Al³⁺.

Taking into account the emerging demand for Ga³⁺ detection and quantification the sensing properties of **MOF 1** towards Ga³⁺ were evaluated in fluorometric titration experiments (Fig. 4c). A linear I-C dependence was observed in the Ga³⁺ concentration range 5–40 μM

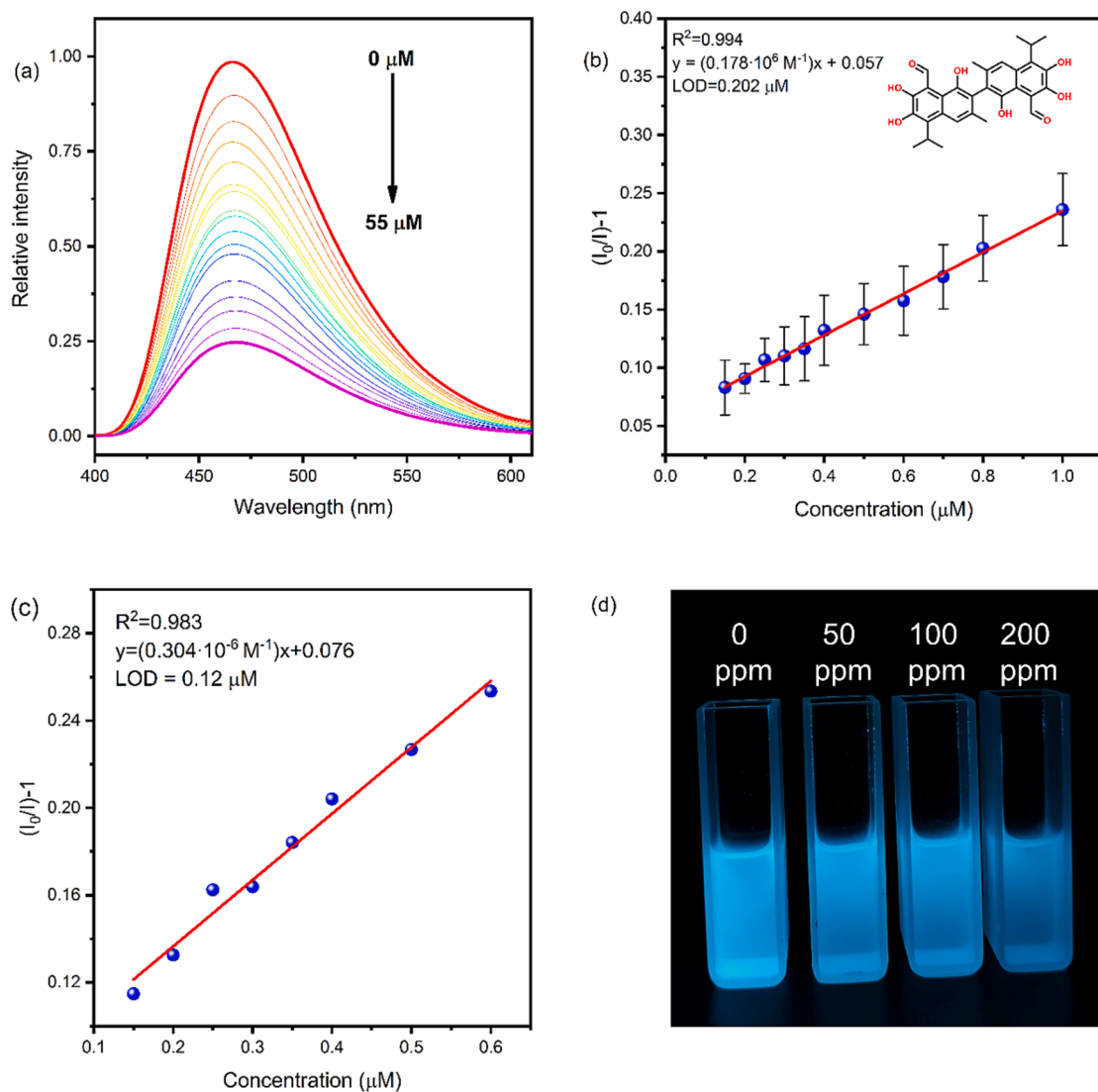


Fig. 3. Luminescent sensing of gossypol by MOF 1: (a) emission spectra of MOF 1 ethanol suspension at different gossypol concentrations ($\lambda_{\text{ex}} 290 \text{ nm}$); (b) linear fit of the concentration-quenching dependance; (c) linear fit of the concentration-quenching dependance with cottonseed oil as background (10 μL in 2 mL); (d) photographs (under 254 nm UV light) of MOF 1 suspensions with 10 μL of sunflower oil added containing different gossypol concentrations. The emission intensities were measured at 470 nm.

(Fig. 4d), from which the limit of detection was determined to be 1.1 μM , which is comparable to the best values reported for Ga^{3+} detection by MOFs (Table S2) (Chai et al., 2022; Li et al., 2022b; Li et al., 2023).

3.3.3. Sensing mechanism

There are several widely recognized mechanisms behind the MOF luminescence quenching by organic analytes: Förster resonance energy transfer (FRET), inner-filter effect (IFE, also known as competitive absorption), collisional quenching, and energy or charge transfer events taking place in the ground or in the excited state.

The possibility of FRET was excluded by comparing the absorption spectrum of gossypol and the emission spectrum of MOF 1 (Figure S14). The absence of overlap between these spectra indicated that the FRET process, i.e., the energy transfer from the excited state of MOF 1 to gossypol molecule is improbable (Mukherjee et al., 2023).

A common approach used for the collisional quenching possibility determination involves calculation of the binding constant, which can be derived using the Stern-Volmer equation. K_{SV} represents the slope in the intensity-concentration linear relationship. Overall, the binding constant can be calculated as $K_q = K_{\text{SV}}/\tau$. The luminescence lifetime (τ) of MOF 1 was ascertained at 15 ns (Figure S15), thus binding constant is

equal to $2.1 \cdot 10^{15} \text{ M}^{-1} \text{ s}^{-1}$, and surpasses the practical threshold for collisional quenching processes (Van De Weert & Stella, 2011).

The possible inner-filter effect can be addressed by ascertaining the analyte's absorbance (Fig. 5a). The UV-Vis absorption spectroscopy was employed to analyze the gossypol solution in ethanol with concentration of 10^{-6} M . Recorded absorbance at 290 nm (0.02) allows us to conclude that the inner-filter effect plays a negligible role in the emission quenching, because degree of emission quenching by gossypol at sub-micromolar concentrations (10^{-7} M) surpasses what can be reasonably ascribed to the absorbance of gossypol (Figure S16). In addition, the UV absorbance of gossypol (at 290 nm) and the quenching efficiency of MOF 1 luminescence (at $\lambda_{\text{ex}} 290 \text{ nm}$) was compared in the concentration range identical to the one used in fluorometric titration (Figure S17). The luminescence quenching efficiency, expressed as I_0/I , was much greater than the absorbance of gossypol, expressed as $1/T$ (T – transmittance of gossypol solution) in the studied concentration range, ruling out the role of IFE in luminescence quenching.

Next, the charge transfer processes were considered. The energy levels of frontier molecular orbitals of the tr_2btd and dcps^{2-} ligands of MOF 1 were calculated using DFT methods and compared to the orbital levels of gossypol calculated at the same level of theory. The HOMO and

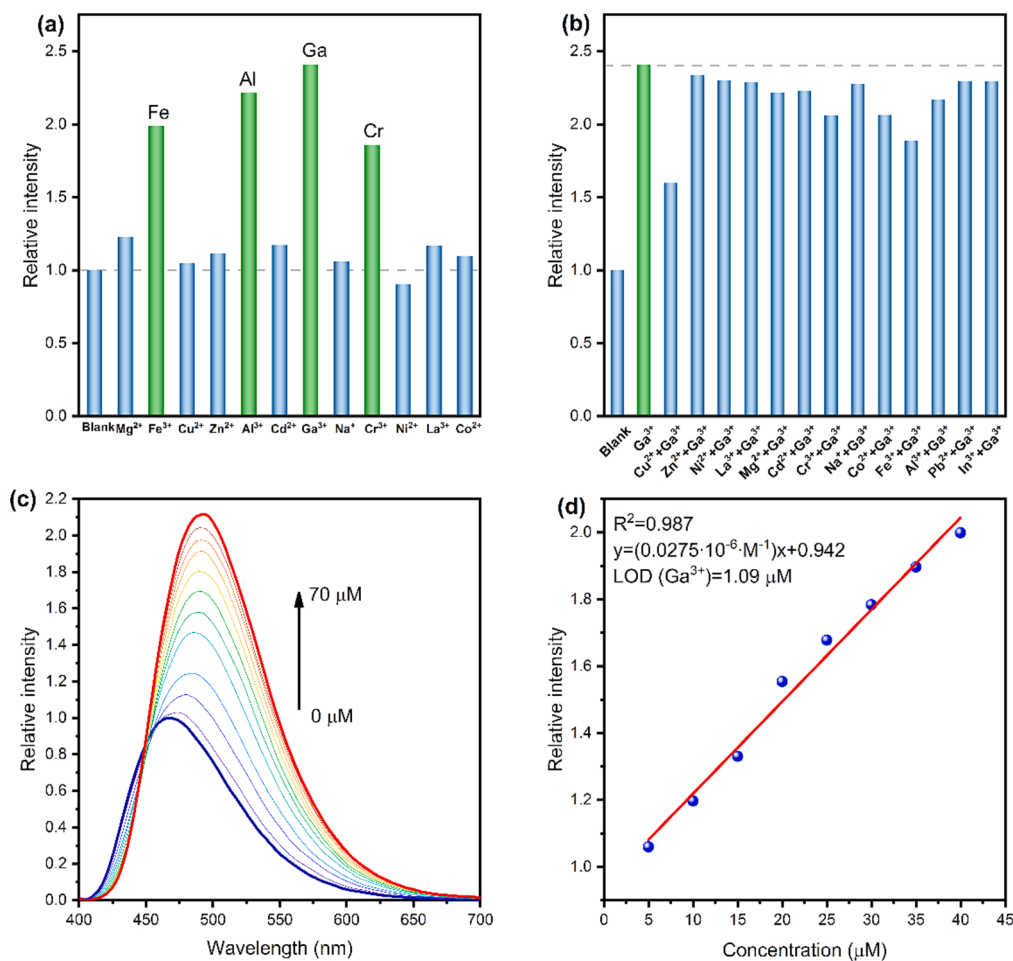


Fig. 4. Luminescent sensing of metal cations by MOF 1: (a) relative integral emission intensities (from 400 to 670 nm) of MOF 1 suspensions in the presence of various metal cations ($C = 1 \cdot 10^{-4}$ M); (b) relative integral emission intensities (from 400 to 670 nm) of MOF 1 suspensions in the simultaneous presence of Ga^{3+} and various metal cations ($C = 1 \cdot 10^{-4}$ M); (c) emission spectra of MOF 1 at different Ga^{3+} concentrations (λ_{ex} 375 nm); (d) linear fit of the concentration-emission intercity dependence.

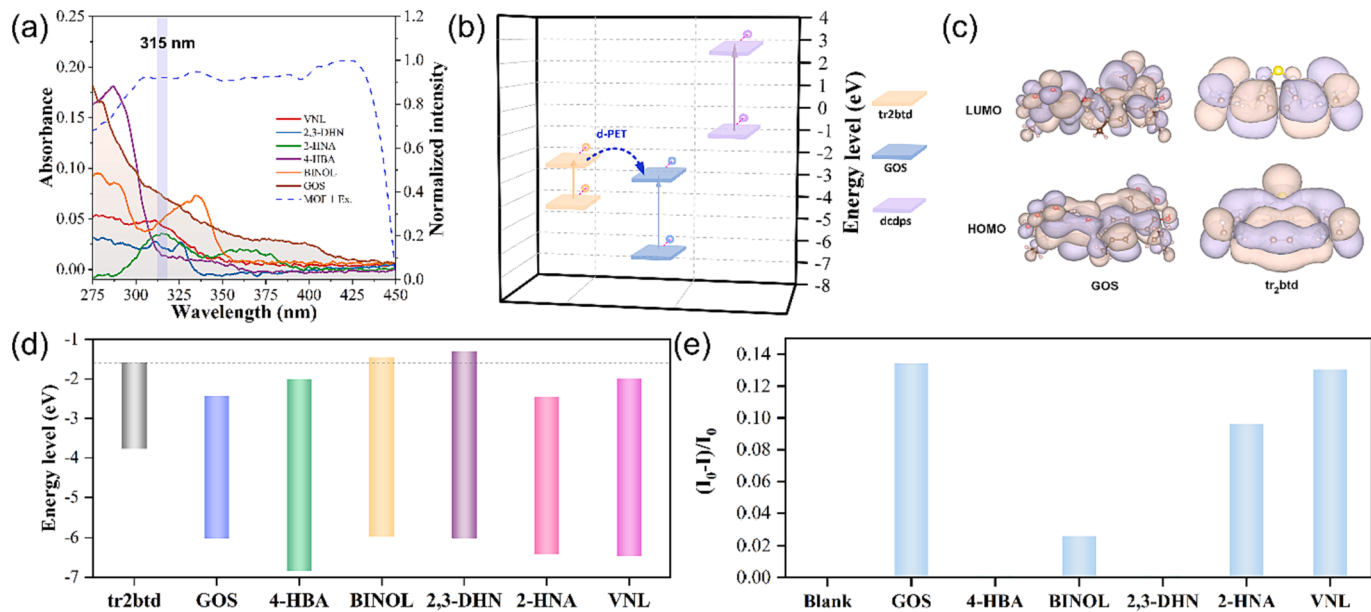


Fig. 5. (a) UV-Vis absorption spectra of gossypol and its chemical analogs in ethanol ($C = 1 \cdot 10^{-5}$ M); (b) energy levels and (c) isosurfaces (at 0.005 e/Bohr³) of HOMO and LUMO orbitals of gossypol (GOS), tr₂btd and dcpc²⁻; (d) HOMO and LUMO energy levels of gossypol chemical analogs; (e) luminescence quenching efficiency of gossypol and its chemical analogs (emission measured at 470 nm and λ_{ex} 290 nm). DFT calculations were carried out at B3LYP 6-311+G(2d,p) level of theory.

LUMO levels of dcps^{2-} are much higher compared to the corresponding orbitals of gossypol (Fig. 5b), therefore the energy transfer between them is improbable. On the contrary, the LUMO level of tr_2btd is comparable to the LUMO level of gossypol, but still higher in energy (Fig. 5b, c) making a d-PET (donor photo-induced electron transfer) process possible (Halder et al., 2023).

In order to get more insight into the role of PET in a row of compounds with functional groups similar to gossypol, a range of aromatic compounds with phenol and aldehyde functional groups were selected (Figure S18): 4-hydroxybenzaldehyde (4-HBA), 1,1'-bi-2-naphthol (BINOL), 2,3-dihydroxynaphthalene (2,3-DHN), 2-hydroxynaphthaldehyde (2-HNA) and 4-hydroxy-3-methoxybenzaldehyde (vanillin, VNL). The UV–Vis absorbance spectra, MOF 1 luminescence quenching efficiency and HOMO/LUMO energy levels of these compounds were evaluated. It was found that two factors are important for the efficient luminescence quenching: (i) LUMO energy level of the analyte lower than the LUMO level of the fluorophore to facilitate the d-PET process; (ii) the presence of the absorption band near the excitation wavelength (315 nm). Thus, among the studied gossypol analogs 2-HNA and VNL have LUMO levels very close to that of gossypol (Fig. 5d) and also a strong UV absorbance at 315 nm (Fig. 5a), these two compounds demonstrated the quenching efficiency comparable to gossypol (Fig. 5e). At the same, 4-HBA has the LUMO level compatible with PET process (Fig. 5d), but only weak absorbance at 315 nm (Fig. 5a), resulting in the absence of the luminescence quenching (Fig. 5e). BINOL has a strong absorbance at 315 nm (Fig. 5a), but the its LUMO level is only slightly higher than that of tr_2btd (Fig. 5d), nevertheless leading to some luminescence quenching. Finally, 2,3-DHN has the LUMO level unfavorable for PET and weak UV absorbance, thus demonstrating no luminescence quenching (Fig. 5e).

As for the luminescence enhancement caused by Ga^{3+} cations, the possible reasons are: structural changes, cation exchange and host–guest interactions with the framework. The structural changes were ruled out by PXRD analysis of MOF 1 sample soaked in Ga^{3+} ethanolic solution. No changes in PXRD pattern were observed compared to the as-synthesized MOF 1 (Figure S19) confirming the structural integrity of the framework. As an additional confirmation, we have recorded the luminescence spectrum of tr_2btd solution with and without Ga^{3+} added and no change of the emission intensity was observed upon addition of Ga^{3+} ions (Figure S20), thus ruling out the emission enhancement through the interaction of Ga^{3+} with the free ligand. Cation exchange in MOF 1 is unlikely, since it is a neutral framework.

A porous structure of MOF 1 and the presence of uncoordinated nitrogen donor atoms in benzo-2,1,3-thiadiazole rings suggests the possibility of interaction between the Ga^{3+} cations and MOF 1 leading to absorbance enhancement which in turn yields the growth of the emission intensity (Karmakar et al., 2019; Pal, 2023). Cyclic sensing experiments revealed that the emission enhancement process is fully reversible (Figure S21), indicating that the interaction of Ga^{3+} with the framework is weak and does not involve the formation of strong coordination bonds.

4. Conclusions

A new metal–organic framework MOF 1 assembled using highly fluorescent ligand 4,7-di(1,2,4-triazol-1-yl)benzo-2,1,3-thiadiazole demonstrated one of the highest photoluminescence quantum yield (74 %) among the transition metal-based MOFs and revealed a multi-responsive luminescent behavior, with a quenching effect towards cotton phytotoxicant gossypol (LOD 0.20 μM) and an enhancement effect to trivalent metal cations (Ga^{3+} , Al^{3+} , Fe^{3+} , LOD for Ga^{3+} 1.1 μM). To the best of our knowledge, MOF 1 is the first luminescent MOF capable of simultaneous detection of gossypol and metal cations (Ga^{3+} , Al^{3+}). As a result of the study of MOF 1 sensing properties we have confirmed the hypothesis that it may be used for distinguishing between the genuine sunflower oil and oil adulterated by crude cottonseed oil through

qualitative and quantitative gossypol determination, which is a natural component of cottonseed products, but should be absent in sunflower and other vegetable oils.

CRediT authorship contribution statement

Dmitry I. Pavlov: Writing – original draft, Methodology, Investigation, Conceptualization. **Xiaolin Yu:** Writing – original draft, Visualization, Investigation. **Alexey A. Ryadun:** Investigation. **Denis G. Samsonenko:** Software, Investigation. **Pavel V. Dorovatovskii:** Software, Investigation. **Vladimir A. Lazarenko:** Software, Investigation. **Na Sun:** Investigation. **Yaguang Sun:** Investigation. **Vladimir P. Fedin:** Software, Investigation. **Andrei S. Potapov:** Writing – review & editing, Project administration, Investigation, Conceptualization.

Declaration of competing interest

The authors declare that they have no known competing financial interests or personal relationships that could have appeared to influence the work reported in this paper.

Data availability

Data will be made available on request.

Acknowledgements

This work was supported by the Russian Science Foundation, grant No. 23-43-00017. Na Sun and Yaguang Sun acknowledge The Belt and Road Innovative Talent Exchange Foreign Experts Program (DL2022006007L). Xiaolin Yu gratefully appreciates the financial support of China Scholarship Council (CSC, grant No. 202008090088) for his postgraduate course at Novosibirsk State University. The authors thank Dr. Konstantin A. Kovalenko for measuring the gas adsorption isotherms.

Appendix A. Supplementary data

Supplementary data to this article can be found online at <https://doi.org/10.1016/j.foodchem.2024.138747>.

References

- Agafonov, M. A., Alexandrov, E. V., Artyukhova, N. A., Bekmukhamedov, G. E., Blatov, V. A., Butova, V. V., Gayfulin, Y. M., Garibyan, A. A., Gafurov, Z. N., Gorbunova, Y. G., Gordeeva, L. G., Gruzdev, M. S., Gusev, A. N., Denisov, G. L., Dybtsev, D. N., Enakieva, Y. Y., Kagilev, A. A., Kanyukov, A. O., Kiskin, M. A., & Yakhvarov, D. G. (2022). Metal-organic frameworks in Russia: From the synthesis and structure to functional properties and materials. *Journal of Structural Chemistry*, 63(5), 671–843. <https://doi.org/10.1134/S0022476622050018>
- Barsukova, M. O., Sapchenko, S. A., Kovalenko, K. A., Samsonenko, D. G., Potapov, A. S., Dybtsev, D. N., & Fedin, V. P. (2018). Exploring the multifunctionality in metal-organic framework materials: How do the stilbenedicarboxylate and imidazolyl ligands tune the characteristics of coordination polymers? *New Journal of Chemistry*, 42(8), 6408–6415. <https://doi.org/10.1039/C8NJ00494C>
- Barthel, S., Alexandrov, E. V., Proserpio, D. M., & Smit, B. (2018). Distinguishing metal-organic frameworks. *Crystal Growth & Design*, 18(3), 1738–1747. <https://doi.org/10.1021/cgd.7b01663>
- Blatov, V. A., Shevchenko, A. P., & Proserpio, D. M. (2014). Applied topological analysis of crystal structures with the program package ToposPro. *Crystal Growth and Design*, 14(7), 3576–3586. <https://doi.org/10.1021/cg500498k>
- Bonneau, C., O'Keeffe, M., Proserpio, D. M., Blatov, V. A., Batten, S. R., Bourne, S. A., Lah, M. S., Eon, J.-G., Hyde, S. T., Wiggins, S. B., & Öhrström, L. (2018). Deconstruction of crystalline networks into underlying nets: relevance for terminology guidelines and crystallographic databases. *Crystal Growth & Design*, 18 (6), 3411–3418. <https://doi.org/10.1021/acs.cgd.8b00126>
- Butova, V. V., Soldatov, M. A., Guda, A. A., Lomachenko, K. A., & Lamberti, C. (2016). Metal-organic frameworks: Structure, properties, synthesis and characterization. *Russian Chemical Reviews*, 85(3), 280–307. <https://doi.org/10.1070/RCR4554>
- Cai, D.-G., Zheng, T.-F., Liu, S.-J., & Wen, H.-R. (2023). Fluorescence sensing and device fabrication of luminescent metal-organic frameworks. *Dalton Transactions*. <https://doi.org/10.1039/D3DT03223J>

- Chai, B.-L., Yao, S.-L., Xie, X., Xu, H., Zheng, T.-F., Li, J.-Y., Chen, J.-L., Liu, S.-J., & Wen, H.-R. (2022). Luminescent metal-organic framework-based fluorescence turn-on and red-shift sensor toward Al³⁺ and Ga³⁺: Experimental study and DFT calculation. *Crystal Growth & Design*, 22(1), 277–284. <https://doi.org/10.1021/acs.cgd.1c00923>
- Chitambar, C. R. (2010). Medical applications and toxicities of gallium compounds. *International Journal of Environmental Research and Public Health*, 7(5), 2337–2361. <https://doi.org/10.3390/ijerph7052337>
- Committee, A. M. (1987). Recommendations for the definition, estimation and use of the detection limit. *The Analyst*, 112(2), 199–204. <https://doi.org/10.1039/AN9871200199>
- Dabbour, M., Hamoda, A., Mintah, B. K., Wahia, H., Betchem, G., Yolandani, Xu, H., He, R., & Ma, H. (2023). Ultrasonic-aided extraction and deglycosylation of cottonseed meal protein: Optimization and characterization of functional traits and molecular structure. *Industrial Crops and Products*, 204, 117261. 10.1016/j.indcrop.2023.117261.
- Directive 2002/32/EC of the European Parliament and of the Council of 7 May 2002 on undesirable substances in animal feed - Council statement.* (2002).
- Dodou, K. (2005). Investigations on gossypol: Past and present developments. *Expert Opinion on Investigational Drugs*, 14(11), 1419–1434. <https://doi.org/10.1517/13543784.14.11.1419>
- Gadelha, I. C. N., Fonseca, N. B. S., Oloris, S. C. S., Melo, M. M., & Soto-Blanco, B. (2014). Gossypol toxicity from cottonseed products. *The Scientific World Journal*, 2014, Article 231635. <https://doi.org/10.1155/2014/231635>
- GB 2716-2018. National food safety standard - Vegetable oil, (2018). <https://www.chinesestandard.net/PDF.aspx/GB2716-2018>.
- Giebelhaus, R. T., Tarazona Carrillo, K., Nam, S. L., de la Mata, A. P., Araneda, J. F., Hui, P., Ma, J., & Harynuk, J. J. (2023). Detection of common adulterants in olive oils by bench top 60 MHz 1H NMR with partial least squares regression. *Journal of Food Composition and Analysis*, 122, 105465. <https://doi.org/10.1016/j.jfca.2023.105465>
- Guan, L., Jiang, Z., Cui, Y., Yang, Y., Yang, D., & Qian, G. (2021). An MOF-based luminescent sensor array for pattern recognition and quantification of metal ions. *Advanced Optical Materials*, 9(9). <https://doi.org/10.1002/adom.202002180>
- Haldar, R., Ghosh, A., & Maji, T. K. (2023). Charge transfer in metal-organic frameworks. *Chemical Communications*, 59(12), 1569–1588. <https://doi.org/10.1039/DCC05522H>
- Han, Z., Wang, K., Zhou, H.-C., Cheng, P., & Shi, W. (2023). Preparation and quantitative analysis of multicenter luminescence materials for sensing function. *Nature Protocols*, 18(5), 1621–1640. <https://doi.org/10.1038/s41596-023-00810-1>
- He, Q. Q., Yao, S. L., Zheng, T. F., Xu, H., Liu, S. J., Chen, J. L., Li, N., & Wen, H. R. (2022). A multi-responsive luminescent sensor based on a stable Eu³⁺ metal-organic framework for sensing Fe³⁺, MnO⁴⁻, and Cr2O⁷²⁻ in aqueous solutions. *CrystEngComm*, 24(5), 1041–1048. <https://doi.org/10.1039/d1ce01503f>
- Hu, J., Yu, B., & Zhou, J. (2023). New generation beta-gallium oxide nanomaterials: growth and performances in electronic devices. *Advanced Engineering Materials*, 25 (19), 2300688. <https://doi.org/10.1002/adem.202300688>
- Ivanoff, C. S., Ivanoff, A. E., & Hottel, T. L. (2012). Gallium poisoning: A rare case report. *Food and Chemical Toxicology*, 50(2), 212–215. <https://doi.org/10.1016/j.fct.2011.10.041>
- Kabsch, W. (2010a). Integration, scaling, space-group assignment and post-refinement. *Acta Crystallographica Section D*, 66(2), 133–144. <https://doi.org/10.1107/S0907444909047374>
- Kabsch, W. (2010b). XDS. *Acta Crystallographica Section D*, 66(2), 125–132. <https://doi.org/10.1107/S0907444909047337>
- Karmakar, A., Samanta, P., Dutta, S., & Ghosh, S. K. (2019). Fluorescent “Turn-on” sensing based on metal-organic frameworks (MOFs). *Chemistry – An Asian Journal*, 14 (24), 4506–4519. <https://doi.org/10.1002/asia.201901168>
- Kokina, T. E., Shekhovtsov, N. A., Vasilyev, E. S., Glinskaya, L. A., Mikheylis, A. V., Plyusnin, V. F., Tkachev, A. V., & Bushuev, M. B. (2023). Efficient emission of Zn(ii) and Cd(ii) complexes with nonplanar-annealed 4,5-diazafuorene and 4,5-diazafuorene-9-one ligands: How slight structural modification alters fluorescence mechanism. *Dalton Transactions*, 52(22), 7429–7446. <https://doi.org/10.1039/D3DT00904A>
- Kumar, M., Tomar, M., Punia, S., Grasso, S., Arrutia, F., Choudhary, J., Singh, S., Verma, P., Mahapatra, A., Patil, S., Radha, Dhumal, S., Potkule, J., Saxena, S., & Amarowicz, R. (2021). Cottonseed: A sustainable contributor to global protein requirements. *Trends in Food Science & Technology*, 111, 100–113. 10.1016/j.tifs.2021.02.058.
- Kumar, M., Zhang, B., Potkule, J., Sharma, K., Radha, Hano, C., Sheri, V., Chandran, D., Dhumal, S., Dey, A., Rais, N., Senapathy, M., Natta, S., Viswanathan, S., Mohankumar, P., & Lorenzo, J. M. (2023). Cottonseed oil: extraction, characterization, health benefits, safety profile, and application. *Food Analytical Methods*, 16(2), 266–280. 10.1007/s12161-022-02410-3.
- Kuznetsova, A., Matveevskaya, V., Pavlov, D., Yakunenkov, A., & Potapov, A. (2020). Coordination polymers based on highly emissive ligands: synthesis and functional properties. *Materials*, 13(12), 2633. <https://doi.org/10.3390/ma13122699>
- Lazarenko, V. A., Dorovatovskii, P. V., Zubavichus, Y. V., Burlov, A. S., Koschienko, Y. V., Vlasenko, V. G., & Khrustalev, V. N. (2017). High-throughput small-molecule crystallography at the ‘Belo’ beamline of the Kurchatov synchrotron radiation source: Transition metal complexes with azomethine ligands as a case study. *Crystals*, 7(11), 325. <https://doi.org/10.3390/crys7110325>
- Li, F., Shaw, S., Libby, C., Preciado, N., Bicer, B., & Tamizhmani, G. (2024). A review of toxicity assessment procedures of solar photovoltaic modules. *Waste Management*, 174, 646–665. <https://doi.org/10.1016/j.wasman.2023.12.034>
- Li, J., Yao, S. L., Zheng, T. F., Xu, H., Li, J. Y., Peng, Y., Chen, J. L., Liu, S. J., & Wen, H. R. (2022a). Turn-on and blue-shift fluorescence sensor toward l-histidine based on stable CdII metal-organic framework with tetrานuclear cluster units. *Dalton Transactions*, 51(15), 5983–5988. <https://doi.org/10.1039/d2dt00390b>
- Li, J., Zhu, Y., Xu, H., Zheng, T.-F., Liu, S.-J., Wu, Y., Chen, J.-L., Chen, Y.-Q., & Wen, H.-R. (2022b). A benzothiadiazole-based Eu³⁺ metal-organic framework as the turn-on luminescent sensor toward Al³⁺ and Ga³⁺ with potential bioimaging application. *Inorganic Chemistry*, 61(8), 3607–3615. <https://doi.org/10.1021/acs.inorgchem.1c03661>
- Li, L. Q., Yao, S. L., Tian, X. M., Zheng, T. F., Li, J. Y., Liu, S. J., Chen, J. L., Yu, M. H., & Wen, H. R. (2021). A fluorescence red-shift and turn-on sensor for acetylacetone derived from ZnII-based metal-organic framework with new topology. *CrystEngComm*, 23(13), 2532–2537. <https://doi.org/10.1039/dice00127b>
- Li, T., Liu, Z., Zhang, Z., Zhang, J., & Zhao, X. (2023). Multiple intrahepatic inflammatory myofibroblastic tumor on 68Ga-FAPI and 18F-FDG PET/CT. *Clinical Nuclear Medicine*, 48(12), e614–e616. https://journals.lww.com/nucarmed/fulltext/2023/12000/multiple_intrahepatic_inflammatory_myofibroblastic.59.aspx
- Li, W., Zhu, J., Qi, X., Sun, C., Li, W., & Chang, Z. (2024). A novel Zn-MOF fluorescent probe for highly sensitive and rapid detection of gossypol in cottonseed oil and fetal bovine serum. *Food Bioscience*, 57, Article 103569. <https://doi.org/10.1016/j.fbio.2023.103569>
- Li, Y., Cai, D. G., Zhu, Z. H., Xu, H., Zheng, T. F., Chen, J. L., Liu, S. J., & Wen, H. R. (2023). Solvothermal synthesis and device fabrication of a Eu³⁺-based metal-organic framework as a turn-on and blue-shift fluorescence sensor toward Cr³⁺, Al³⁺ and Ga³⁺. *Dalton Transactions*, 52(13), 4167–4175. <https://doi.org/10.1039/d2dt003230a>
- Li, Y., Chai, B.-L., Xu, H., Zheng, T.-F., Chen, J.-L., Liu, S.-J., & Wen, H.-R. (2022). Temperature- and solvent-induced reversible single-crystal-to-single-crystal transformations of TbIII-based MOFs with excellent stabilities and fluorescence sensing properties toward drug molecules. *Inorganic Chemistry Frontiers*, 9(7), 1504–1513. <https://doi.org/10.1039/DQI00023G>
- Lin, J.-L., Fang, X., Li, J.-X., Chen, Z.-W., Wu, W.-K., Guo, X.-X., Liu, N.-J., Huang, J.-F., Chen, F.-Y., Wang, L.-J., Xu, B., Martin, C., Chen, X.-Y., & Huang, J.-Q. (2023). Dirigent gene editing of gossypol enantiomers for toxicity-depleted cotton seeds. *Nature Plants*, 9(4), 605–615. <https://doi.org/10.1038/s41477-023-01376-2>
- Liu, Y., Wang, L., Zhao, L., & Zhang, Y. (2022). Structure, properties of gossypol and its derivatives—from physiological activities to drug discovery and drug design. *Natural Product Reports*, 39(6), 1282–1304. <https://doi.org/10.1039/DINP00080B>
- Liu, Y., Xie, X. Y., Cheng, C., Shao, Z. S., & Wang, H. S. (2019). Strategies to fabricate metal-organic framework (MOF)-based luminescent sensing platforms. *Journal of Materials Chemistry C*, 7(35), 10743–10763. <https://doi.org/10.1039/c9tc03208h>
- Lyu, W., Ding, M., Zhou, Y., Jiang, M., Li, Y., Ding, Y., Zhang, Z., Wei, X., & Zhang, X. (2023). A highly sensitive electrochemical sensor for capsaicinoids and its application in the identification of illegal cooking oil. *Biosensors*, 13(9), 863. <https://doi.org/10.3390/bios13090863>
- Ma, D., Li, B., Zhou, X., Zhou, Q., Liu, K., Zeng, G., Li, G., Shi, Z., & Feng, S. (2013). A dual functional MOF as a luminescent sensor for quantitatively detecting the concentration of nitrobenzene and temperature. *Chemical Communications*, 49(79), 8964–8966. <https://doi.org/10.1039/c3cc44546a>
- Mohan, B., Priyanka, Singh, G., Chauhan, A., Pombeiro, A. J. L., & Ren, P. (2023). Metal-organic frameworks (MOFs) based luminescent and electrochemical sensors for food contaminant detection. *Journal of Hazardous Materials*, 453, 131324. 10.1016/j.jhazmat.2023.131324.
- Mukherjee, S., Sarkar, K., & Biswas, S. (2023). A fluorophore anchored MOF for fast and sensitive sensing of Cu(II) and 3-nitrotyrosine in a physiological medium. *Dalton Transactions*, 52(17), 5597–5605. <https://doi.org/10.1039/D3DT00660C>
- Muthukumar, R., Kapoor, A., Balasubramanian, S., Vaishampayan, V., & Gabhane, M. (2021). Detection of adulteration in sunflower oil using paper-based microfluidic lab-on-a-chip devices. *Materials Today: Proceedings*, 34, 496–501. <https://doi.org/10.1016/j.matpr.2020.03.099>
- Ninkuu, V., Liu, Z., Zhou, Y., & Sun, X. (2023). The nutritional and industrial significance of cottonseeds and genetic techniques in gossypol detoxification. *PLANTS, PEOPLE, PLANET*, n/a(n/a), 1–16. 10.1002/ppp3.10433.
- Pal, T. K. (2023). Metal-organic framework (MOF)-based fluorescence “turn-on” sensors. *Materials Chemistry Frontiers*, 7(3), 405–441. <https://doi.org/10.1039/D2QM01070D>
- Pavlov, D. I., Ryadun, A. A., & Potapov, A. S. (2021). A Zn(II)-based sql type 2D coordination polymer as a highly sensitive and selective turn-on fluorescent probe for Al³⁺. *Molecules*, 26(23), 7392. <https://doi.org/10.3390/molecules26237392>
- Pavlov, D. I., Yu, X., Ryadun, A. A., Fedin, V. P., & Potapov, A. S. (2023). Luminous metal-organic framework with 2,1,3-benzothiadiazole units for highly sensitive gossypol sensing. *Chemosensors*, 11(1), 52. <https://doi.org/10.3390/chemosensors11010052>
- Percy, R. G., Calhoun, M. C., & Kim, H. L. (1996). Seed gossypol variation within Gossypium barbadense L. cotton. *Crop Science*, 36(1), 193–197. <https://doi.org/10.2135/cropsci1996.0011183X003600010034x>
- Puttha, R., Venkatachalam, K., Hanpakdeesakul, S., Parametthanuwat, T., Srean, P., Pakeechai, K., & Charoenphon, N. (2023). Exploring the potential of sunflowers: agronomy, applications, and opportunities within bio-circular-green economy. *In Horticulturae*, 9(10), 1079. <https://doi.org/10.3390/horticulturae9101079>
- Raj, P. S., Bergfeld, W. F., Belsito, D. V., Cohen, D. E., Klaassen, C. D., Liebler, D. C., Rettie, A. E., Ross, D., Slaga, T. J., Snyder, P. W., Tilton, S., Fiume, M., & Heldreth, B. (2023). Cottonseed glyceride and hydrogenated cottonseed glyceride. *International Journal of Toxicology*, 42(3 suppl), 27S–28S. 10.1177/10915818231204275.
- Rizzo, A., Miceli, A., Racca, M., Bauckheit, M., Morbelli, S., Albano, D., Dondi, F., Bertagnia, F., Galizia, D., Muoio, B., Annunziata, S., & Treglia, G. (2023). Diagnostic accuracy of [68Ga] Ga labeled fibroblast-activation protein inhibitors in detecting head and neck cancer lesions using positron emission tomography: A systematic

- review and a meta-analysis. *Pharmaceuticals*, 16(12). <https://doi.org/10.3390/ph16121664>, 1664.
- Salah, W. A., & Nofal, M. (2021). Review of some adulteration detection techniques of edible oils. *Journal of the Science of Food and Agriculture*, 101(3), 811–819. <https://doi.org/10.1002/jsfa.10750>
- Sheldrick, G. M. (2015a). Crystal structure refinement with SHELXL. *Acta Crystallographica Section C*, 71(1), 3–8. <https://doi.org/10.1107/S2053229614024218>
- Sheldrick, G. M. (2015b). SHELXT - Integrated space-group and crystal-structure determination. *Acta Crystallographica Section A*, 71(1), 3–8. <https://doi.org/10.1107/S2053273314026370>
- Sing, K. S. W., Everett, D. H., Haul, R. A. W., Moscou, L., Pierotti, R. A., Rouquerol, J., & Siemieniewska, T. (1985). Reporting physisorption data for gas/solid systems with special reference to the determination of surface area and porosity. *Pure and Applied Chemistry*, 57(4), 603–619. <https://doi.org/10.1351/pac198557040603>
- Spek, A. L. (2015). PLATON SQUEEZE: A tool for the calculation of the disordered solvent contribution to the calculated structure factors. *Acta Crystallographica Section C*, 71(1), 9–18. <https://doi.org/10.1107/S2053229614024929>
- Stefanidis, S., Ordoudi, S. A., Nenadis, N., & Pyrka, I. (2023). Improving the functionality of virgin and cold-pressed edible vegetable oils: Oxidative stability, sensory acceptability and safety challenges. *Food Research International*, 174, Article 113599. <https://doi.org/10.1016/j.foodres.2023.113599>
- Svetogorov, R. D., Dorovatovskii, P. V., & Lazarenko, V. A. (2020). Belok/XSA diffraction beamline for studying crystalline samples at Kurchatov synchrotron radiation source. *Crystal Research and Technology*, 55(5), 1900184. <https://doi.org/10.1002/crat.201900184>
- Tan, C. H., Kong, I., Irfan, U., Solihin, M. I., & Pui, L. P. (2021). Edible oils adulteration: A review on regulatory compliance and its detection technologies. *Journal of Oleo Science*, 70(10), 1343–1356. <https://doi.org/10.5650/jos.ess21109>
- Tian, M., Bai, Y., Tian, H., & Zhao, X. (2023). The chemical composition and health-promoting benefits of vegetable oils—A review. In *Molecules* (Vol. 28, Issue 17, p. 6393). 10.3390/molecules28176393.
- Tian, X. M., Yao, S. L., Qiu, C. Q., Zheng, T. F., Chen, Y. Q., Huang, H., Chen, J. L., Liu, S. J., & Wen, H. R. (2020). Turn-on luminescent sensor toward Fe³⁺, Cr³⁺, and Al³⁺ based on a Co(II) metal-organic framework with open functional sites. *Inorganic Chemistry*, 59(5), 2803–2810. <https://doi.org/10.1021/acs.inorgchem.9b03152>
- Tranchemontagne, D. J., Mendoza-Cortés, J. L., O'Keeffe, M., & Yaghi, O. M. (2009). Secondary building units, nets and bonding in the chemistry of metal-organic frameworks. *Chemical Society Reviews*, 38(5), 1257. <https://doi.org/10.1039/b817735j>
- Van De Weert, M., & Stella, L. (2011). Fluorescence quenching and ligand binding: A critical discussion of a popular methodology. *Journal of Molecular Structure*, 998 (1–3), 144–150. <https://doi.org/10.1016/J.MOLSTRUC.2011.05.023>
- Vilela, J., Coelho, L., & de Almeida, J. M. M. M. (2015). Investigation of adulteration of sunflower oil with thermally deteriorated oil using Fourier transform mid-infrared spectroscopy and chemometrics. *Cogent Food & Agriculture*, 1(1), 1020254. <https://doi.org/10.1080/23311932.2015.1020254>
- Wang, Y., Cao, J., Wang, G., Wei, T., Hu, K., Yi, W., Zeng, P., Li, H., Wu, Y., & He, Q. (2023). Synthesis and characterization of zeolitic imidazole frameworks nanocrystals and their application in adsorption and detoxification of gossypol in cottonseed oil. *Food Chemistry*, 418, Article 135905. <https://doi.org/10.1016/j.foodchem.2023.135905>
- White, S. J. O., & Shine, J. P. (2016). Exposure potential and health impacts of indium and gallium, metals critical to emerging electronics and energy technologies. *Current Environmental Health Reports*, 3(4), 459–467. <https://doi.org/10.1007/s40572-016-0118-8>
- Xu, X., Li, X., Xu, Z., Yang, H., Lin, X., & Leng, X. (2024). Replacing fishmeal with cottonseed protein concentrate in practical diet of largemouth bass (*Micropterus salmoides*): Growth, flesh quality and metabolomics. *Aquaculture*, 579, Article 740164. <https://doi.org/10.1016/j.aquaculture.2023.740164>
- Yakar, Y., & Karadag, K. (2022). Identifying olive oil fraud and adulteration using machine learning algorithms. *Quimica Nova*, 45(10), 1245–1250. <https://doi.org/10.21577/0100-4042.20170948>
- Yang, R., Yu, X., Xu, B., Yao, W., Fedin, V. P., Potapov, A. S., & Gao, E. (2023). A novel 3D hexagonal honeycomb Zn-MOF for effective detection of Fe³⁺, CrO4²⁻, and Cr2O7²⁻ and selective dye adsorption in aqueous media. *Polyhedron*, 243, Article 116535. <https://doi.org/10.1016/j.poly.2023.116535>
- Yao-Say Solomon Adade, S., Lin, H., Jiang, H., Haruna, S. A., Osei Barimah, A., Zareef, M., et al. (2022). Fraud detection in crude palm oil using SERS combined with chemometrics. *Food Chemistry*, 388, 132973. 10.1016/j.foodchem.2022.132973.
- Yao, S. L., Xiong, Y. C., Tian, X. M., Liu, S. J., Xu, H., Zheng, T. F., Chen, J. L., & Wen, H. R. (2021). A multifunctional benzothiadiazole-based fluorescence sensor for Al³⁺, Cr³⁺ and Fe³⁺. *CrystEngComm*, 23(9), 1898–1905. <https://doi.org/10.1039/D1CE00060H>
- Ye, Y., Khushvakov, J., Boboev, A., Akramova, R., Yunusov, O., Dalimova, D., Turdikulova, S., Mirzaakhmedov, S., Engelsen, S. B., & Khakimov, B. (2022). Effect of refinement and production technology on the molecular composition of edible cottonseed oils from a large industrial scale production. *Journal of Functional Foods*, 99, Article 105326. <https://doi.org/10.1016/j.jff.2022.105326>
- Yili Prefecture Market Supervision and Administration Bureau Administrative Penalty Decision Letter Yizhou City Supervision Penalty [2022] No. 27, b4ef4c000/2023 (2022). <https://www.xjyl.gov.cn/xjylz/c112662/202301/0caf9269e43427fa60b96e4116130de.shtml>
- Yu, X., Gao, E., Yao, W., Fedin, V. P., & Potapov, A. S. (2022a). Zinc(II) and cobalt(II) complexes with unusual coordination of mixed imidazole-1,2,4-triazole ligand in a protonated cationic form. *Polyhedron*, 217, Article 115741. <https://doi.org/10.1016/j.poly.2022.115741>
- Yu, X., Pavlov, D. I., Ryadun, A. A., Potapov, A. S., & Fedin, V. P. (2022b). Variable dimensionality of Europium(III) and Terbium(III) coordination compounds with a flexible hexacarboxylate ligand. *Molecules*, 27(22), 7849. <https://doi.org/10.3390/molecules27227849>
- Yu, X., Ryadun, A. A., Kovalenko, K. A., Guselnikova, T. Y., Ponomareva, V. G., Potapov, A. S., & Fedin, V. P. (2023a). 4 in 1: Multifunctional Europium-organic frameworks with luminescence sensing properties, white light emission, proton conductivity and reverse acetylene-carbon dioxide adsorption selectivity. *Dalton Transactions*, 52(25), 8695–8703. <https://doi.org/10.1039/d3dt01323e>
- Yu, X., Ryadun, A. A., Potapov, A. S., & Fedin, V. P. (2023b). Ultra-low limit of luminescent detection of gossypol by terbium(III)-based metal-organic framework. *Journal of Hazardous Materials*, 452, Article 131289. <https://doi.org/10.1016/j.jhazmat.2023.131289>
- Zaukuu, J.-L.-Z., Abaidoo-Ayin, L., Bimpong, D., Amponsah, L. A., & Mensah, E. T. (2024). Predictive techniques for authenticating and quantifying crude palm oil adulterated with leaf extract and food color – An ultra-violet visible spectrophotometric approach. *Journal of Food Composition and Analysis*, 126, Article 105895. <https://doi.org/10.1016/j.jfca.2023.105895>
- Zhan, T., Xu, M., Cao, Z., Zheng, C., Kurita, H., Narita, F., Wu, Y.-J., Xu, Y., Wang, H., Song, M., Wang, W., Zhou, Y., Liu, X., Shi, Y., Jia, Y., Guan, S., Hanajiri, T., Maekawa, T., Okino, A., & Watanabe, T. (2023). Effects of thermal boundary resistance on thermal management of gallium-nitride-based semiconductor devices: A review. *Micromachines*, 14(11), 2076. <https://doi.org/10.3390/mi14112076>